LETTERS
PUBLISHED ONLINE: 17 MAY 2009 | DOI: 10.1038/NPHYS1278
nature physics

Wave–particle duality of single surface plasmon polaritons

Roman Kolesov[1], Bernhard Grotz[1], Gopalakrishnan Balasubramanian[1], Rainer J. Stöhr[1], Aurélien A. L. Nicolet[1], Philip R. Hemmer[2], Fedor Jelezko[1]* and Jörg Wrachtrup[1]*

When light interacts with metal surfaces, it excites electrons, which can form propagating excitation waves called surface plasmon polaritons. These collective electronic excitations can produce strong electric fields localized to subwavelength distance scales[1], which makes surface plasmon polaritons interesting for several applications. Many of these potential uses, and in particular those related to quantum networks[2], require a deep understanding of the fundamental quantum properties of surface plasmon polaritons. Remarkably, these collective electron states preserve many key quantum mechanical properties of the photons used to excite them, including entanglement[3,4] and sub-Poissonian statistics[5]. Here, we show that a single-photon source coupled to a silver nanowire excites single surface plasmon polaritons that exhibit both wave and particle properties, similar to those of single photons. Furthermore, the detailed analysis of the spectral interference pattern provides a new method to characterize the dimensions of metallic waveguides with nanometre accuracy.

One of the most intriguing experiments of contemporary physics is the double-slit self-interference of single particles. Among the possible quantum systems, photons seem to be ideal for such demonstrations because of their ability to propagate long distances in ambient environment, yet still be efficiently detected. A key requirement for photon self-interference experiments is the availability of a true single-photon source. Light sources such as lasers show intrinsic fluctuation of photon numbers related to Poissonian statistics. Hence, the outcome of double-slit experiments with such light sources can be described classically without introducing the concept of photons (a quantized electromagnetic field)[6]. In the benchmark study realized two decades ago by Grangier and co-workers, true single-photon states emitted from an atomic cascade revealed a clear interference pattern[7,8]. Like photons, surface plasmon polaritons can be used for Young double-slit experiments[9], and the recent generation of single plasmons by single quantum emitters opens the door for studying their fundamental quantum properties[5]. Here, both antibunching and self-interference are observed using single plasmons excited by a single-photon emitter, and this unambiguously shows that the concept of single-particle self-interference can be applied to surface plasmon polaritons. As this interference arises from an *in situ* interferometer wherein one beam splitter is the bi-directional emission into the nanowire, and the other beam splitter is the partially transmitting wire output end, it also provides a sensitive diagnostic method to determine nanowire properties. In addition, by choosing spin-selective nitrogen-vacancy colour centres in diamond as the single-photon emitters, we open the door to eventually achieving strong coupling between spins and plasmons, for which applications include single-shot spin readout for room-temperature quantum computers and nano-magnetometers.

To generate non-classical states of surface plasmon polaritons, single colour centres in diamond nanocrystals were coupled to metallic waveguides. Single nitrogen-vacancy colour centres in diamond were chosen as the emitters because of their absolute photostability at room temperature. Crystalline, chemically grown silver wires were used as waveguides because of the low loss in silver in the visible spectral range. Nitrogen-vacancy emitters were placed in the near-field of the nanowires by mixing a diamond nanocrystal solution with the silver wires, and spin-coating the resulting nanodiamond-coated wires onto a glass substrate (for details of the sample preparation, see the Methods section). Figure 1a shows an atomic force microscopy (AFM) image of diamond nanocrystals attached to the surface of a nanowire. Surprisingly, an efficient self-assembly process leads to sticking of single nanodiamond particles to wires (see the AFM picture). The inset shows the fluorescence image of the same wire with bright spots originating from emission of single nitrogen-vacancy defects. The size of the diamond nanocrystals was about 50 nm and the average distance between the emitter and the metal is expected to be of the order of 25 nm. As a result of being placed in close proximity to the metallic surface, the nitrogen-vacancy defects show a significant reduction of their fluorescence lifetime owing to efficient coupling of the excited nitrogen-vacancy emission to surface plasmon polaritons. Enhanced decay rates of the emitter due to excitation of surface plasmons are the most important effect for distances between the metal surface and the nitrogen-vacancy centre within the range of 10–100 nm (ref. 10). As the coupling is a near-field effect, it depends on the distance between the surface of the wire and each nitrogen-vacancy defect, and on the orientation of the nitrogen-vacancy emission dipole with respect to the axis of the wire. The enhanced coupling is apparent from the analysis of the Purcell factor for a collection of different nanocrystals (see Fig. 1). On average, we observe a Purcell factor of 2.5, which is in good agreement with the theoretically predicted value[5] for an emitter–wire separation of 30 nm. In general, the coupling efficiency depends on the wire radius R as $1/R^3$; that is, stronger coupling is expected for thinner wires[11]. However, the plasmon to photon conversion efficiency at the wire ends and the plasmon propagation length increase with increasing R. Hence, for the present experiment, an average wire diameter of 70 nm was found to be a good compromise, enabling efficient emitter coupling while keeping losses low and photon outcoupling high. Coupling of single-photon sources to plasmonic waveguides was reported previously for quantum dots[5,12].

A single-photon emitter coupled to the metal wire is an ideal test system that provides experimental access to the statistical properties

[1]3. Physikalisches Institut, Universität Stuttgart, 70550 Stuttgart, Germany, [2]Department of Electrical and Computer Engineering, Texas A&M University, 77843 College Station, USA. *e-mail: f.jelezko@physik.uni-stuttgart.de; wrachtrup@physik.uni-stuttgart.de.

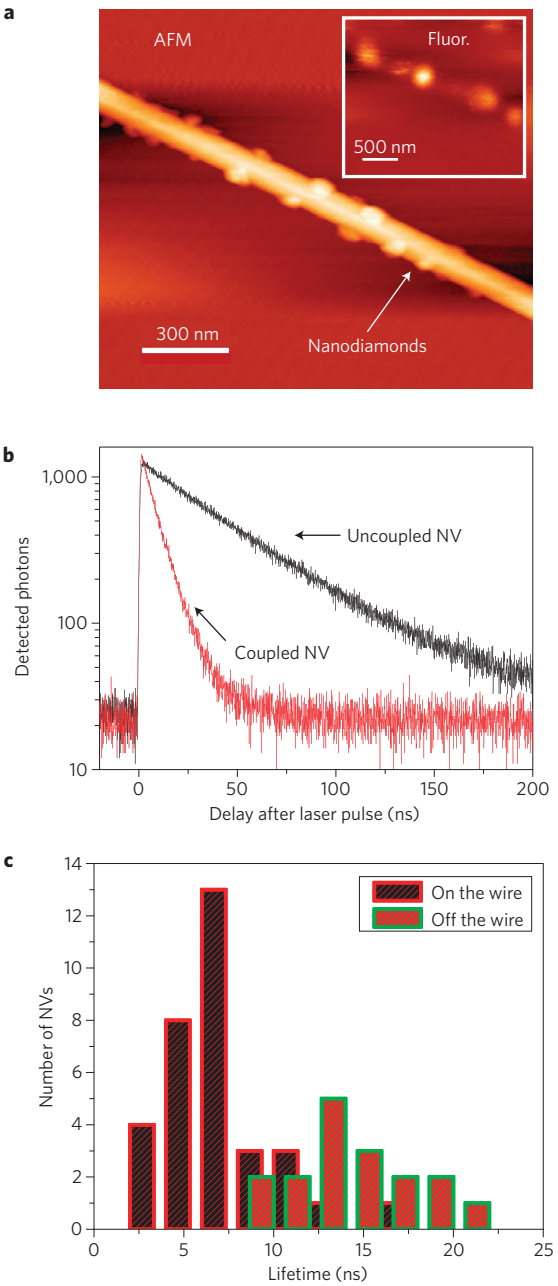

Figure 1 | Single-photon emitter coupled to a silver wire. a, AFM image of diamond nanocrystals attached to a silver nanowire. Inset: The fluorescence image of the wire, with bright spots corresponding to the emission of single nitrogen-vacancy (NV) defects. **b**, Fluorescence lifetime measurements of nitrogen-vacancy defects coupled to silver wire (red line). Fluorescence decay of isolated nanocrystals containing nitrogen-vacancy defects is also shown (black line). **c**, Distribution of fluorescence lifetimes for single-photon nitrogen-vacancy emitters coupled to the wire, showing an average Purcell factor of 2.5.

of single surface plasmon polaritons. The generic experimental arrangement for such an experiment with photons is shown in the upper panel of Fig. 2a. A single-photon wave packet originating from the non-classical source is divided on a beam splitter. The two detectors on the output of the beam splitter record coincidence events. Assuming that the reflectivity of the beam splitter is a constant quantity, the coincidence rate for a classical 'wave' description follows the inequality $P_C \geq P_1 P_2$, where P_1 and P_2 are the probabilities of detecting a photon by either of the two detectors. The quantum mechanical description predicts $P_C = P_1 P_2$ for a Poissonian source, $P_C = 2P_1 P_2$ for a thermal source and $P_C = 0$ for a source of single photons[6]. The detection of a single photon projects the optical emitter into the ground state because of energy conservation. Hence, it is impossible to detect a second photon simultaneously. As the $P_C = 0$ case corresponds to a photon at one detector or the other, but never both, it demonstrates the particle-like propagation of single photons. Similar experiments can be realized for surface plasmon polaritons, as shown in the lower panel of Fig. 2a. When the plasmon excitation reaches the end of the wire, it can be coupled to an optical photon that propagates to a detector in the far-field. Hence, coincidence analysis for photons coupled out at both ends of the wire enables us to measure the second-order intensity autocorrelation function of surface plasmon polaritons.

Figure 2b shows the wide-field image of a silver plasmonic waveguide when the laser beam is focused on a single nitrogen-vacancy defect coupled to the wire. Both ends of the wire show detectable fluorescence, indicating the propagation of plasmons along the wire. To check that single surface plasmon polaritons are excited by the single-photon source, measurements of the second-order correlation function are carried out between both ends of the wire (see Fig. 2c). The absence of the peak at zero delay time provides experimental proof that the plasmons originate from the fluorescence of a single quantum system. It is remarkable that even though a surface plasmon involves a large number of electrons, it behaves like a single quantum particle. As a control experiment, coincidence measurements were also carried out between nitrogen-vacancy defect emission to free space and the end of the wire, which corresponds to the joint detection of a photon and a plasmon. Near-perfect anticorrelation was observed, indicating that the contribution of background light coupled out at the wire end is negligible. Although this photon–plasmon anticorrelation does not demonstrate the particle-like properties of the plasmon, it is important to mention that it indicates that the silver waveguide conserves the non-classical statistics of the diamond single-photon source, in agreement with a previous observation for a quantum dot emitter[5]. Finally, photon correlation measurements were carried out on the emission of the nitrogen-vacancy itself. The absence of the peak at zero delay verifies that the emitter is in fact a single nitrogen vacancy.

The next step is to observe the wave-like properties of a single-plasmon polariton, which provides evidence for 'wave–particle duality'. Quantum mechanical interference of single photons occurs when there are different trajectories for the photons—for example in a Mach–Zehnder interferometer—that contribute to the photon detection probability at the output. The detectors at the two outputs of the interferometer show a modulation in count rate, when the path difference of the interferometer arms is varied (see Fig. 3a). This experiment was adapted for single-plasmon self-interference as follows. A single nitrogen-vacancy emitter coupled to a one-dimensional wire is equally likely to excite a plasmon propagating in either direction and hence the emitter–plasmon coupling also serves as the first beam splitter. The plasmon propagating to the left in Fig. 3a reflects off the end of the wire and interferes with the plasmon emitted to the right. Hence, the right half of the wire acts as the second beam splitter. Although the length of the wire waveguide cannot be changed, the path length and dispersion enables the interference at the end of the wire to be observed because the different spectral components of the single-plasmon wave packet acquire different phases by the time they reach the end[13]. The nitrogen-vacancy defect is particularly suitable for such spectral self-interference owing to its broadband emission (see the upper spectrum of Fig. 3b). The intensity of the plasmonic field at the exit of the waveguide is given by

$$I(\omega) = E_1(\omega)^2 + E_2(\omega)^2 + 2E_1(\omega)E_2(\omega)\cos[2k(\omega)d + \phi_R]$$

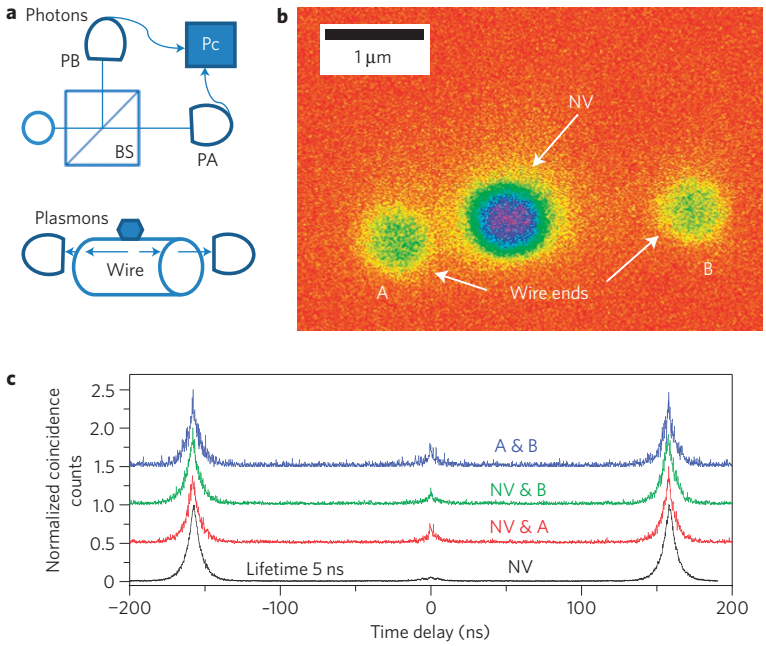

Figure 2 | Sub-Poissonian statistics of single surface plasmon polaritons. a, The Hanbury Brown–Twiss experiment for single photons (top) and single surface plasmon polaritons (bottom). PA/PB: photodiode A/B; Pc: photon correlator; BS: beam splitter. **b**, The fluorescence image of a single quantum emitter (optically excited single nitrogen-vacancy defect in diamond) coupled to a silver wire. **c**, Second-order intensity correlation function of a single-photon nitrogen-vacancy emitter in the far-field (black line). The missing coincidence peak at zero delay time indicates that the emission is originating from a single nitrogen-vacancy defect. When the coincidence is recorded between the nitrogen-vacancy defect photon and either end of the wire, the missing peak at zero delay indicates that single surface plasmon polaritons originating from the single-photon source are coupled out at the ends of the wire (red and green lines). The blue line shows the measurement of cross-correlation between the two ends of the wire. Here, the missing peak at zero delay is proof of the particle-like behaviour of single surface plasmon polaritons.

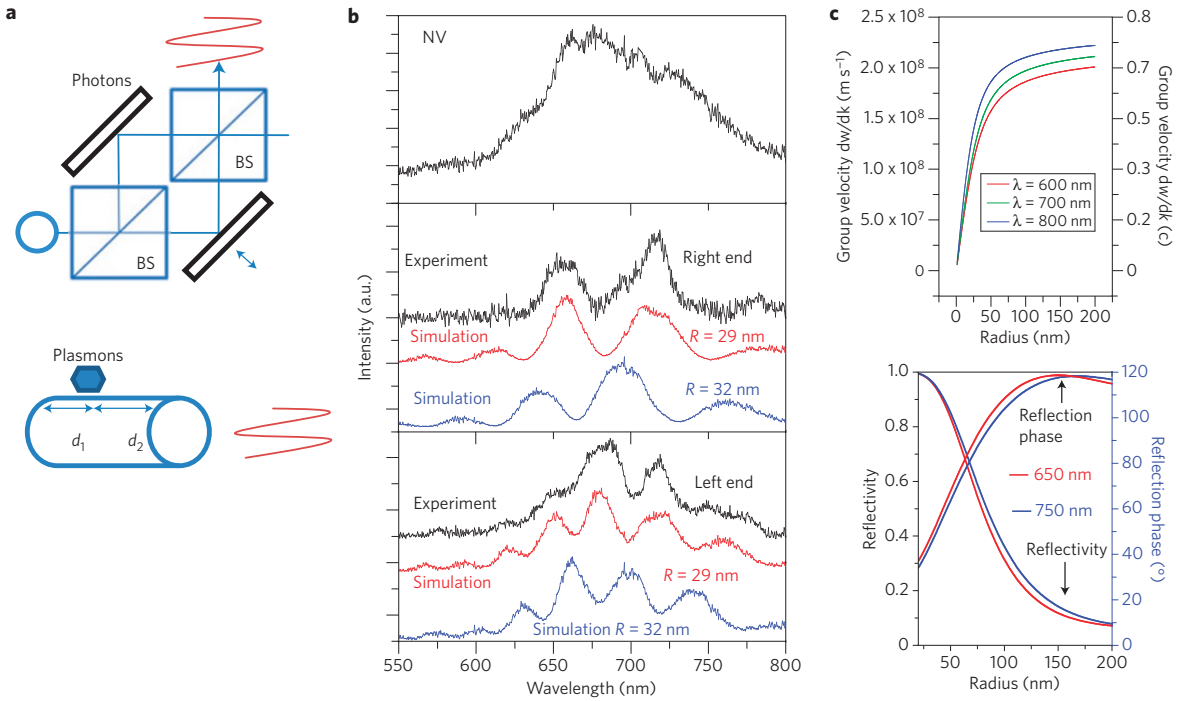

Figure 3 | Self-interference of single surface plasmon polaritons. a, Diagram showing single-photon (top) and single-plasmon (bottom) self-interference experiments. **b**, Fluorescence emission spectra of a single nitrogen-vacancy centre (top) and of single plasmons coupled out from the ends of the wire (two bottom graphs, black curves). The red lines show results of simulations taking into account losses during propagation of plasmons in the wire as well as dispersion for wire radius $R = 29$ nm. The blue lines are results of simulations for wire radius $R = 32$ nm. **c**, Spectral dependence of the group velocity of surface plasmon polaritons for three different wire diameters (top graph). The bottom graph shows numerical simulations of the reflection coefficient and the reflection phase for two different wavelengths covering the range of nitrogen-vacancy emission (details of the calculations are given in Supplementary Information).

Here E_1 and E_2 are the amplitudes associated with the field propagating directly to the end of the wire from the nitrogen-vacancy emitter and the field reflecting off the other end of the wire, d is the distance between the nitrogen-vacancy centre and the end of the wire, $k(\omega)$ is the surface plasmon wave vector and ϕ_R is the phase shift experienced by the surface plasmon polariton under reflection. Figure 3b shows the interference patterns observed for both output ends of the wire. Both spectra demonstrate strong modulation when compared with direct emission of the nitrogen-vacancy defect, which is consistent with a simple picture describing a silver nanowire as a lossy cavity[14–16]. Owing to propagation losses, the contrast of interference fringes is lower for emission from the left end of the wire because $d_2 > d_1$. The distances d_2 and d_1 could be directly determined from the confocal picture. Thus, setting $E_1 = E_0 e^{-\alpha d_1}$ and $E_2 = E_0 e^{-\alpha(d_1+2d_2)}$, one can calculate the ratio of $(E_1/E_2) = e^{2\alpha d_2}$ for a given damping factor α, where d_1 and d_2 are the distances between the nitrogen-vacancy centre and the close and far end of the wire (marked as ends A and B in Fig. 3), respectively. To describe the observed interference pattern, we have calculated the group velocity (see Fig. 3c) and phase acquired by the surface plasmon polariton on reflection (see Supplementary Information and ref. 17 for details). Remarkably, the reflection coefficient of the wire end is expected to be close to unity for wire with a radius smaller than 40 nm, which is in good agreement with the high contrast of the experimentally observed interference fringes. As the wire radius becomes larger, the reflectivity of the wire end drops to ≈2%. The reflection phase, which scales linearly with the wire radius R relevant for our experiments ($R = 30$ nm), approaches 120° for large R, which is consistent with the results obtained previously for a semi-infinite metal slab[18]. Fitting of the observed spectra is very sensitive to the wire diameter (see the simulated spectra in Fig. 2b) owing to its influence on the reflection phase shift and the strong dispersion (see Fig. 3c). It is important to mention that the fitting results are unique when the interference pattern observed for both ends of the wire is taken into consideration. Hence, single-photon interference enables the determination of the wire diameter with an accuracy of better than 1 nm. Note that such characterization of plasmonic structures has an advantage compared with AFM or electron microscopy because interferometry enables measurement of the effective optical dimensions of the waveguide with long standoff distances and under ambient conditions.

The two experiments presented here demonstrate wave–particle duality of single surface plasmon polaritons. Particle behaviour is observed in the antibunching experiments, whereas the wave picture is required for the description of the self-interference. The intrinsic conflict between those two classical interpretations is at the heart of quantum mechanics. It was shown recently that quantum behaviour is preserved during photon to plasmon conversion even though surface plasmon polaritons involve a macroscopic number of metal electrons[4]. Here, it is important to note that nitrogen-vacancy defects in diamonds, which are used to generate single surface plasmon polaritons, are one of the most attractive candidates for solid-state qubits, because their ground-state spin can be initialized and readout optically[19] and the number of quantum operations per coherence time is unusually large, even at room temperature[20,21]. Hence, this demonstration of efficient coupling of nitrogen-vacancy centres to single surface plasmon polaritons potentially opens the door to the use of metallic waveguides for coupling distant nitrogen-vacancy defects as required for maximum scalability. Cooperative phenomena such as superradiance mediated by surface plasmons were discussed in the literature[22,23] and long distance coupling of single quantum emitters through plasmonic modes was suggested recently[24]. Thus, single plasmons on metal nanowires can provide a powerful tool to couple numerous multi-qubit diamond quantum registers[25], in which, for example, three-qubit entanglement was demonstrated recently[26], to fabricate large-scale room-temperature quantum processors.

Methods

Silver nanowires were synthesized using a polyol process[27]. The synthesis started by heating 5 ml ethylene glycol (Baker) in a 25 ml Erlenmeyer flask under 260 r.p.m. stirring at 151.5 °C in an oil bath, and solutions of hydrated cupric chloride ($CuCl_2(H_2O)_2$, Aldrich), silver nitrate $AgNO_3$ (Aldrich) and polyvinylpyrrolidone (PVP, molecular weight ~55,000, Aldrich) were prepared. 47.9 mg of $AgNO_3$, 49 mg of PVP and 2.0 mg of $CuCl_2(H_2O)_2$ were dissolved in 3 ml of ethylene glycol each. After 60 min, 40 µl of the cupric chloride solution was added to the heated ethylene glycol. Fifteen minutes later, 1.5 ml of the PVP solution and immediately after that 1.5 ml of the $AgNO_3$ solution were dropped into the hot ethylene glycol. The reaction ran for a further 90 min, until the flask was allowed to cool down to room temperature. The crude product was washed three times in acetone (Aldrich) to remove the ethylene glycol. Then, the nanowires were dispersed in water for further measurements. This method of treatment did not destroy the polymer coating of the wires that resulted from the growth process. Samples were prepared by spin-coating a solution of nanodiamonds (MSY 0–0.05 Mikron GAF, microndiamant AG Switzerland) and silver nanowires dispersed in water onto a plasma-cleaned glass slide in air. The nanodiamonds stuck to the polymer coating of the wires without any intentional surface treatment. Fluorescence measurements were carried out using a home-built confocal microscope. A pulsed 532 nm Nd:Yag laser was used as the excitation source and was focused onto the sample using a 1.35-numerical-aperture oil-immersion objective, and a second mirror-scanning optical path was used to generate the second confocal detection spot.

To calculate the group velocity $d\omega/dk$ as a function of wire radius R, a model consisting of a metallic cylinder with a dielectric constant ε_2 surrounded by a dielectric medium of dielectric constant ε_1 was used. The surface plasmon propagation in this case is governed by the dispersion relation for the fundamental transverse magnetic mode, which is given by[17]:

$$\frac{k_2^2}{k_{2\perp}}\frac{J_0'(k_{2\perp}R)}{J_0(k_{2\perp}R)} - \frac{k_1^2}{k_{1\perp}}\frac{H_0'(k_{1\perp}R)}{H_0(k_{1\perp}R)} = 0 \qquad (1)$$

where $k_i = (\sqrt{\varepsilon_i}\omega/c) = \sqrt{k_{i\perp}^2 + k_{i\parallel}^2}$ and J_m, H_m are Bessel and Hankel functions of the first kind, respectively. By numerically solving the above equation (1), we can compute the group velocity as a function of R for a given frequency ω and given ε_1 and ε_2.

The value for ε_1 of the surrounding medium is predominantly determined by the glass cover slip and was therefore set to 1.4. In the range of interest from 1.39 eV (892 nm) to 2.26 eV (548.6 nm), the values for $\varepsilon_{2,\mathrm{real}}$ (ref. 28) were fitted with a second-order polynomial function yielding to $\varepsilon_{2,\mathrm{real}}(\omega) = -160.5 + 8.06 \times 10^{-14} \times \omega - 1.10 \times 10^{-29} \times \omega^2$. As in this range, $\varepsilon_{2,\mathrm{img}}$ is two orders of magnitude smaller than $\varepsilon_{2,\mathrm{real}}$, this part was neglected for the calculation of $d\omega/dk$ as a function of R and the determination of the positions of the interference maxima and minima.

Received 19 September 2008; accepted 16 April 2009; published online 17 May 2009

References

1. Barnes, W. L., Dereux, A. & Ebbesen, T. W. Surface plasmon subwavelength optics. *Nature* **424**, 824–830 (2003).
2. Chang, D. E., Sørensen, A. S., Demler, E. A. & Lukin, M. D. A Single-photon transistor using nanoscale surface plasmons. *Nature Phys.* **3**, 807–812 (2007).
3. Altewischer, E., van Exter, M. P. & Woerdman, J. P. Plasmon-assisted transmission of entangled photons. *Nature* **418**, 304–306 (2002).
4. Fasel, S. *et al.* Energy-time entanglement preservation in plasmon-assisted light transmission. *Phys. Rev. Lett.* **94**, 110501 (2005).
5. Akimov, A. V. *et al.* Generation of single optical plasmons in metallic nanowires coupled to quantum dots. *Nature* **450**, 402–406 (2007).
6. Loudon, R. Non-classical effects in the statistical properties of light. *Rep. Prog. Phys.* **43**, 913–949 (1980).
7. Aspect, A. & Grangier, P. Wave-particle duality for single photons. *Hyperfine Interactions* **37**, 3–18 (1987).
8. Grangier, P., Roger, G. & Aspect, A. Experimental-evidence for a photon anticorrelation effect on a beam splitter—a new light on single-photon interferences. *Europhys. Lett.* **1**, 173–179 (1986).
9. Zia, R. & Brongersma, M. L. Surface plasmon polariton analogue to Young's double-slit experiment. *Nature Nanotech.* **2**, 426–429 (2007).
10. Ford, G. W. & Weber, W. H. Electromagnetic-interactions of molecules with metal-surfaces. *Phys. Rep.* **113**, 195–287 (1984).
11. Chang, D. E., Sørensen, A. S., Hemmer, P. R. & Lukin, M. D. Quantum optics with surface plasmons. *Phys. Rev. Lett.* **97**, 053002 (2006).

12. Fedutik, Y., Temnov, V. V., Schops, O., Woggon, U. & Artemyev, M. V. Exciton-plasmon-photon conversion in plasmonic nanostructures. *Phys. Rev. Lett.* **99**, 136802 (2007).
13. Temnov, V. V., Woggon, U., Dintinger, J., Devaux, E. & Ebbesen, T. W. Surface plasmon interferometry: Measuring group velocity of surface plasmons. *Opt. Lett.* **32**, 1235–1237 (2007).
14. Allione, M., Temnov, V. V., Fedutik, Y., Woggon, U. & Artemyev, M. V. Surface plasmon mediated interference phenomena in low-Q silver nanowire cavities. *Nano Lett.* **8**, 31–35 (2008).
15. Ditlbacher, H. *et al.* Silver nanowires as surface plasmon resonators. *Phys. Rev. Lett.* **95**, 257403 (2005).
16. Laroche, T. & Girard, C. Near-field optical properties of single plasmonic nanowires. *Appl. Phys. Lett.* **89**, 233119 (2006).
17. Chang, D. E., Sorensen, A. S., Hemmer, P. R. & Lukin, M. D. Strong coupling of single emitters to surface plasmons. *Phys. Rev. B* **76**, 035420 (2007).
18. Gordon, R. Vectorial method for calculating the Fresnel reflection of surface plasmon polaritons. *Phys. Rev. B* **74**, 153417 (2006).
19. Gruber, A. *et al.* Scanning confocal optical microscopy and magnetic resonance on single defect centers. *Science* **276**, 2012–2014 (1997).
20. Childress, L. *et al.* Coherent dynamics of coupled electron and nuclear spin qubits in diamond. *Science* **314**, 281–285 (2006).
21. Gaebel, T. *et al.* Room-temperature coherent coupling of single spins in diamond. *Nature Phys.* **2**, 408–413 (2006).
22. Bonifacio, R. & Morawitz, H. Cooperative emission of an excited molecular monolayer into surface-plasmons. *Phys. Rev. Lett.* **36**, 1559–1562 (1976).
23. Temnov, V. V. & Woggon, U. Superradiance and subradiance in an inhomogeneously broadened ensemble of two-level systems coupled to a low-Q cavity. *Phys. Rev. Lett.* **95**, 243602 (2005).
24. Durach, M., Rusina, A., Klimov, V. & Stockman, M. Nanoplasmonic renormalization and enhancement of Coulomb interactions. *New J. Phys.* **10**, 105011 (2008).
25. Dutt, M. V. G. *et al.* Quantum register based on individual electronic and nuclear spin qubits in diamond. *Science* **316**, 1312–1316 (2007).
26. Neumann, P. *et al.* Multipartite entanglement among single spins in diamond. *Science* **320**, 1326–1329 (2008).
27. Korte, K., Skrabalak, S. & Xia, Y. Rapid synthesis of silver nanowires through a CuCl- or $CuCl_2$-mediated polyol process. *J. Mater. Chem.* **8**, 437–441 (2008).
28. Johnson, P. B. & Christy, R. W. Optical-constants of noble-metals. *Phys. Rev. B* **6**, 4370–4379 (1972).

Acknowledgements

We would like to thank Ralf Vogelgesang for helpful discussions. This work was supported by the EU (QAO, EQUIND, NEDQIT), DFG (SFB/TR21 and FOR730), Landesstiftung BW, NIH and DARPA.

Author contributions

R.K., B.G., G.B., R.J.S. and A.A.L.N. carried out the experiments; P.R.H., F.J. and J.W. designed and coordinated the experiments; and F.J. wrote the paper. All authors discussed the results, analysed the data and commented on the manuscript.

Additional information

Supplementary information accompanies this paper on www.nature.com/naturephysics. Reprints and permissions information is available online at http://npg.nature.com/reprintsandpermissions. Correspondence and requests for materials should be addressed to F.J. or J.W.